Ocean Science Journal, Vol. 40 No. 4, 213-220(2005)

Note

Ocean Science Journal

http://osj.kordi.re.kr

Image Processing for Video Images of Buoy Motion

Baeck Oon Kim[1]* and Hong Yeon Cho[2]

[1]*Saemangeum Environmental Research Center, Kunsan National University, Kunsan 573-701, Korea*
[2]*Coastal Disaster Prevention Research Division, KORDI, Ansan P.O. Box 29, Seoul 425-600, Korea*

Received 22 November 2005; Revised 6 December 2005; Accepted 12 December 2005

Abstract – In this paper, image processing technique that reduces video images of buoy motion to yield time series of image coordinates of buoy objects will be investigated. The buoy motion images are noisy due to time-varying brightness as well as non-uniform background illumination. The occurrence of boats, wakes, and wind-induced white caps interferes significantly in recognition of buoy objects. Thus, semi-automated procedures consisting of object recognition and image measurement aspects will be conducted. These offer more satisfactory results than a manual process. Spectral analysis shows that the image coordinates of buoy objects represent wave motion well, indicating its usefulness in the analysis of wave characteristics.

Key words – image processing, video image, object recognition, feature measurement, wave direction

1. Introduction

A field experiment was accompanied with video monitoring in the period of June 18-19, 1999 at the East Sea Ocean Research Center of Seoul National University in order to take wave measurements by way of video images of buoy motion. A camcorder (Samsung SV-H66), installed on the third floor of the building (see Fig. 3a in Kim *et al.* 1998; Fig. 4a in Kim 2005), was aimed at two white and red colored buoys deployed at a depth of 8 m (Fig. 1). The white buoy, in particular, was equipped with a 3 m long pole, a weight, and a flag. A total of 9 runs were conducted at an hour interval and each run produced a video record of 8.6 min in duration (Table 1).

To obtain wave characteristics from video images of buoy motion, it is necessary to develop photogrammetry that converts image coordinates of buoy objects to the ground coordinates of the buoy. The time series of the ground coordinates of the buoy can be regarded as a proxy of water surface movement. Thus, an image processing of extracting image coordinates of buoy objects from video records is a prerequisite in the analysis and of major concern in this study.

It is noted that image processing techniques for buoy motion images are different from the techniques that yield time-stacked images for the analysis of coastal processes (*e.g.* Lippmann and Holman 1989; Holman *et al.* 1993). The buoy motion images should be treated individually to extract the image coordinates of buoy objects from each frame. Subsequently, the extracted coordinates are compiled into time-series data. This frame-by-frame process appears to be trivial because buoy objects are visually identifiable as shown in Fig. 1. However, the problem comes from computerized or automated processes because they are required to deal with a large amount of video images. These computerized processes of object recognition may be affected more seriously by the noise and quality of each frame than by time stacking methods. As it turns out, efficiency of computerized processes was highly dependent on factors encountered in field conditions. Thus, success in terms of automated image processing must play a fundamental role in developing a real-time process of data reduction: conversion of 2-D images into an array of image coordinates.

The objective of this study is to investigate the properties of buoy motion images as to what controls an automated process for object recognition as well as image measurement. Considering the image properties and the

*Corresponding author. E-mail: bkim@kunsan.ac.kr

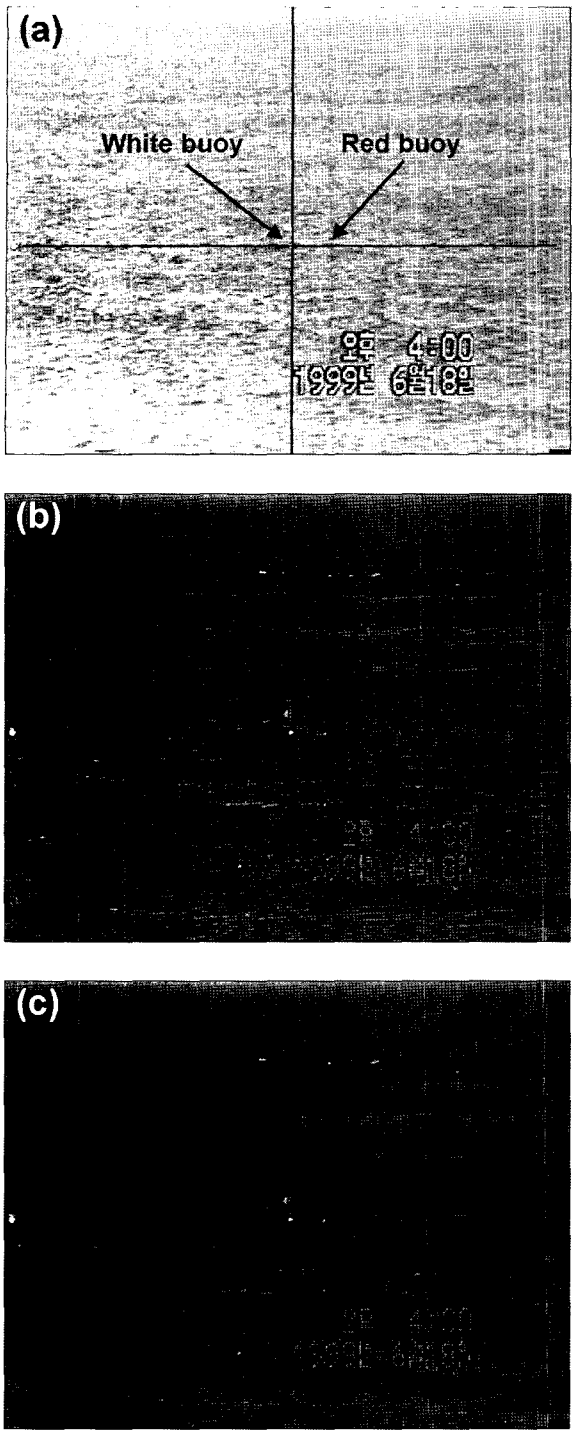

Fig. 1. Video images in the course of image enhancement: (a) original, (b) contrast, and (c) filtered.

current stage of our technology, we are confident about recommending semi-automated procedures. The Matlab program, especially for image processing toolbox, is used for the development of all the procedures (MathWorks 2001). This method is evaluated in comparison with the time-consuming manual process.

2. Methods

Digital images

Using a PC equipped with a graphic driver (Radeon, ATI Technologies Inc.), analog video records were digitized into a sequence of digital images. This instrument system is able to capture digital images of a standard 640×480 array of pixels up to the rate of 29.9 frames/sec. For each 8.6 min video record, a total of 1,024 video frames were captured at 0.5 sec intervals (*i.e.* 2 frames/sec) and stored into an AVI format file. Thereafter, the AVI file was disassembled into 1,024 individual image files of JPEG format, whose names are arranged in numeric sequence.

Image properties

Fig. 1a shows a typical 256-gray-scale image, in which both white and red buoy objects are visible. Thus, image coordinates of buoy objects can be determined manually, but a large number of image files and subjectiveness of the manual process demand an automated procedure.

Intensity profiles along vertical and horizontal transects depicted in Fig. 1a show that white buoy object is the strongest intensity feature (Figs. 2a and b). Image background is characterized by non-uniform and wavelike illumination due to waves reflecting the sun. Also, image brightness varies with the sun's altitude. These image properties may complicate the identification process of the strongest feature. To improve image quality, images are treated with a contrast adjustment process and then applied to a Weiner filter. As shown in Fig. 2, background intensities in enhanced images are significantly subdued in comparison with those in the original images. On the other hand, strong intensity features such as white and red buoy objects do not show any noticeable change. Figs. 1b and c illustrate images according to a series of image enhancement processes.

More difficult problems come from unexpected image properties that are inevitable in field experiments. Occasionally, buoy motion images contain strong intensity features other than buoy objects. These features include boats, wakes, flags and white caps as exemplified in Fig. 3. It is obvious that their occurrence affects the automated process of recognizing the buoy objects. In addition, there are a few

Table 1. Results of object recognition.

Run	Date	Time	Missing	Interfering objects				Total
				Flag	Wakes	White caps	Background	
1	6-18	15:30	3	0	9	1	2	15
2		16:00	3	17	39	0	5	64
3		17:00	5	13	0	14	1	33
4		18:00	17	9	0	49	10	85
5		19:00	16	1	0	2	37	56
6	6-19	07:00	-	-	-	-	-	-
7		08:00	25	0	17	0	21	63
8		09:00	11	0	0	0	4	15
9		10:00	5	0	4	0	6	15

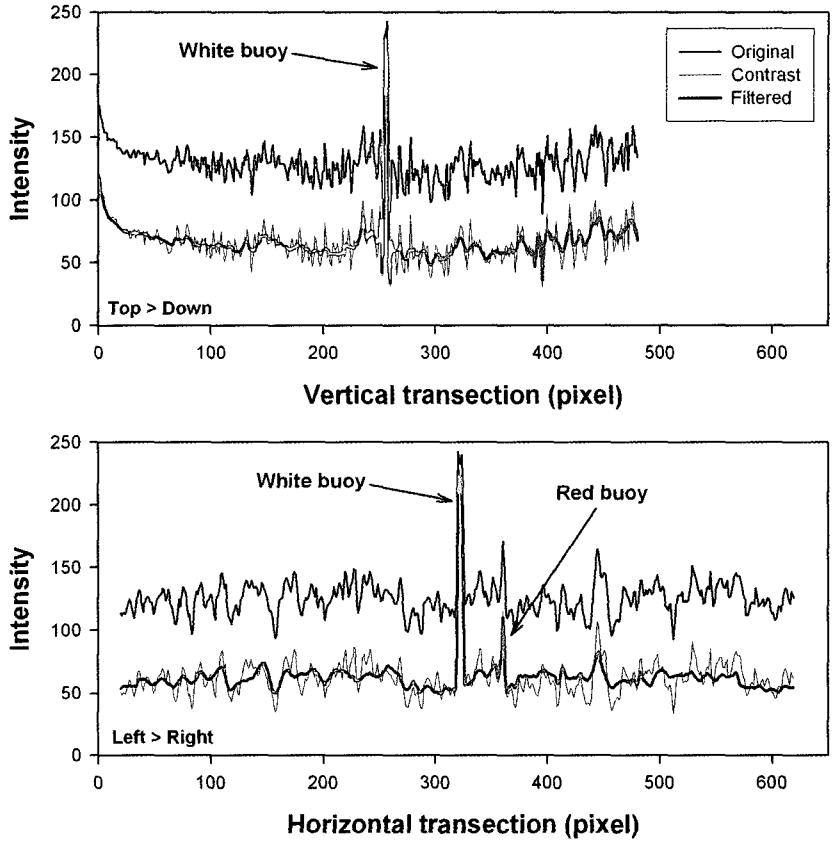

Fig. 2. Intensity profiles in vertical and horizontal transections of video image.

cases where buoy objects are missing or look too vague to be distinguished from their surroundings. For this reason, we attempt to build a semi-automated procedure that reduces massive data as follows.

Image processing

Overall image processing is divided into two parts: object recognition and image measurement (Fig. 4). The object recognition part yields preliminary results for locations of buoy objects as well as information on what kind of strong intensity features interfere with the computerized identification of buoy objects. These results assist in determining the region of interest in the image measurement aspect, from which object features can be analyzed more precisely.

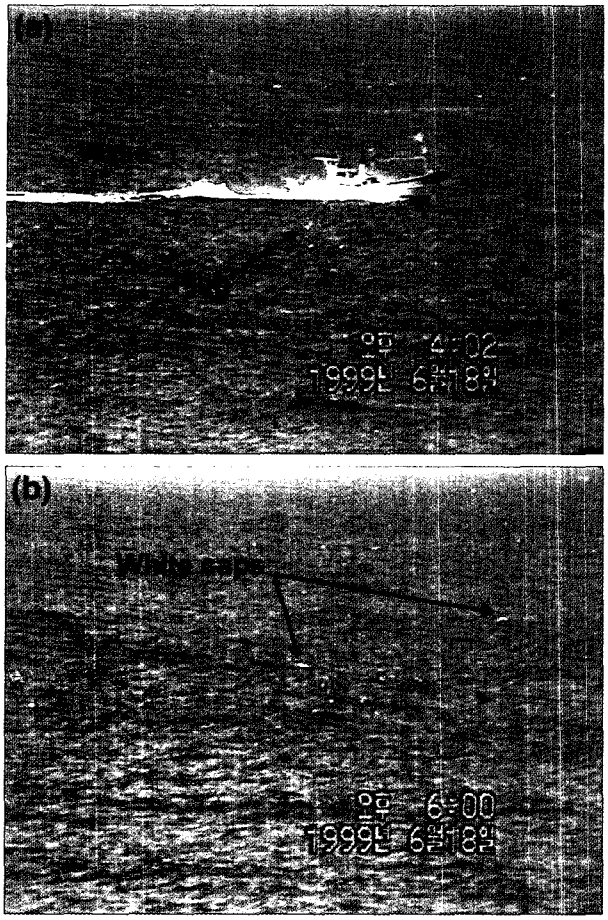

Fig. 3. Examples of video images having unexpected objects: (a) boat, wake and flag, (b) white caps.

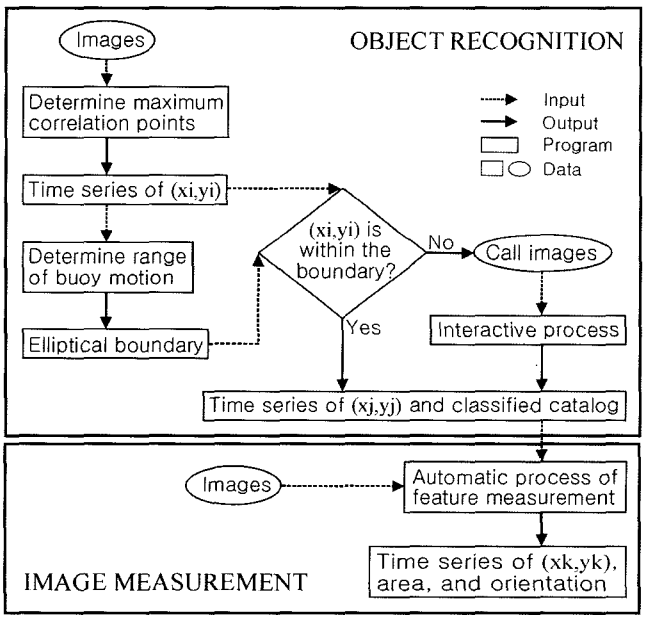

Fig. 4. Flow chart of image processing.

Object recognition

The object recognition aspect consists of three programs. It starts with a program that calculates image coordinates of buoy object location, (xi, yi) based on image intensity. Images are cropped to a certain size covering the range of buoy displacements, which excludes most of the irrelevant background (Fig. 5a). The cropped images are enhanced as described in the previous section. To remove objects larger than buoy objects, a rank filter of [5, 5] size is applied and then image difference operation is conducted. Finally, a correlation matrix of the same image size is made using a two-dimensional operator, which is given as

$$\begin{bmatrix} 0 & 1 & 0 \\ 1 & 1 & 1 \\ 0 & 1 & 0 \end{bmatrix}$$

Fig. 5a exemplifies the image of the correlation matrix, where the image coordinates of the maximum correlation value is set to the buoy object location.

The intensity-based image processing is not always successful because there are some cases where interfering objects show maximum correlation values. Instead of developing a more complicated process considering other aspects of imaging such as color, we attempt here to revise false results and analyze their image properties using a simple tool. In fact, most of correct locations tend to concentrate on a small area due to the limited range of buoy motion as shown in Fig. 5b. The second program is used for determining an elliptical boundary to define the community of correct locations. Alternatively, this process can be performed visually.

In the third program, coordinates of buoy objects are judged in comparison with the elliptical boundary (Fig. 4). An interactive process deals with only images against which the comparison decides and evaluates them in two stages. In the first stage, the user assigns conditional values (0=missing and -1=wrong position) to each image according to whether the buoy object is missing. All the images that pass the comparison have a conditional value of 1. Images having a conditional value of -1 go into the second stage, which manually relocates buoys in a misallocated position to the true buoy object position and examines what competes with the buoy object. Another set of conditional values is allocated to the interfering objects such as flags, wakes, white caps and backgrounds.

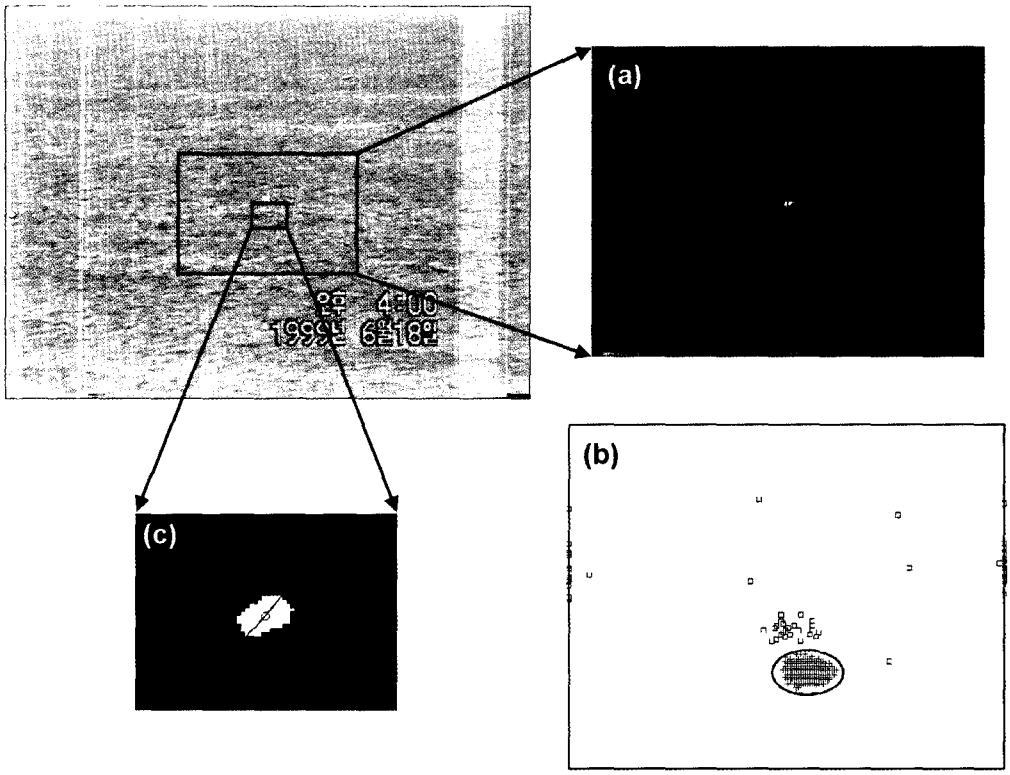

Fig. 5. Cropped images resulted from (a) object recognition and (c) image measurement processes. (b) shows the results of object recognition.

The category background indicates that the buoy object is so faint that its surroundings have much larger intensity. In the missing cases, image coordinates of buoy objects are inserted by interpolation. As a result, the image recognition data reveals the time series of the revised buoy object position, (xj, yj) and two kinds of conditional values.

Image measurement

Since approximate locations of buoy objects are known, each image is cropped to the region of interest, *i.e.*, to the extent that it contains only the buoy object without any interfering objects (Fig. 5c). This region of interest is interpolated to half a pixel unit in order to double the precision of object feature measurement. Then, the region of interest is transformed into a binary image using a threshold value given by half the intensity range, *i.e.*, 0.5× (Maximum intensity - Minimum intensity). Following the procedures as described in Russ (1990), the object area, equivalent diameter of area, centroid and orientation are calculated (Fig. 5c). It is the centroid of the buoy object feature that makes the time series data of the image coordinates of the buoy object, (xk, yk) except for images that have no buoy object. Especially for the missing case, the position due to the image recognition data, (xj, yj) is adopted as the image coordinate of the buoy object without the feature measurement process.

3. Results and Discussion

One way to evaluate image processing technique, counts taken of missing and interfering objects and averaged values of feature measurement parameters are summarized in Tables 1 and 2. It is noted that other image processing techniques might give different results. Video records of run 6 are excluded from the analysis due to poor image quality. Approximately four percent of images are processed manually (Table 1). Both background and missing cases occur all the time, but they have a much higher score late in the afternoon (run 4 to 5) and early in the morning (run 7). It seems that background and missing cases are affected by low altitude of the sun. On the other hand, interference due to flag and white caps is noticeable only in the afternoon, although the flag is

Table 2. Averaged values of image measurement parameters over the run. Values in parenthesis denote standard deviation.

Run	Threshold	Area (pixel^2)	Diameter (pixel)	Orientation (°)
1	125.7(4.1)	15.0(2.9)	4.4(0.4)	17.0(8.5)
2	123.9(3.5)	18.8(3.0)	4.9(0.4)	18.3(9.2)
3	124.9(3.5)	18.3(3.2)	4.8(0.4)	20.8(11.9)
4	125.1(3.6)	16.0(3.4)	4.6(0.5)	22.7(14.5)
5	123.2(9.5)	12.3(2.2)	4.0(0.4)	17.9(21.6)
7	100.3(8.5)	8.3(1.6)	3.2(0.3)	-26.8(18.9)
8	123.5(5.4)	9.1(1.5)	3.4(0.3)	-23.7(13.7)
9	130.9(4.5)	11.8(1.7)	3.9(0.3)	-13.1(7.6)

flapping in most cases and white caps occur occasionally over the experiment (see Fig. 3). This implies that the direction of the sun may play an important role. As for wakes, they do interfere regardless of the sun's altitude and direction only if they occur. In this respect, wakes appear to be the strongest interfering object. This result shows that video imagery has time-dependent property to control image processing.

Relatively narrow ranges of average and standard deviation of threshold values, except for run 7, indicate that cropped image intensity in the image measurement is more or less constant (Table 2). Hence, the area or equivalent diameter of a buoy object is expected to be uniform. However, the buoy object is larger in the afternoon than in the morning. As shown in Fig. 5c, the buoy object has an elliptical shape and its orientation changes with time: positive in the afternoon, but negative in the morning. This instance shows that buoy object size changes with the sun's direction. Again, the time-related property of video images is responsible for the outcome of the feature measurement.

Fig. 6 depicts an example of the time-series of the

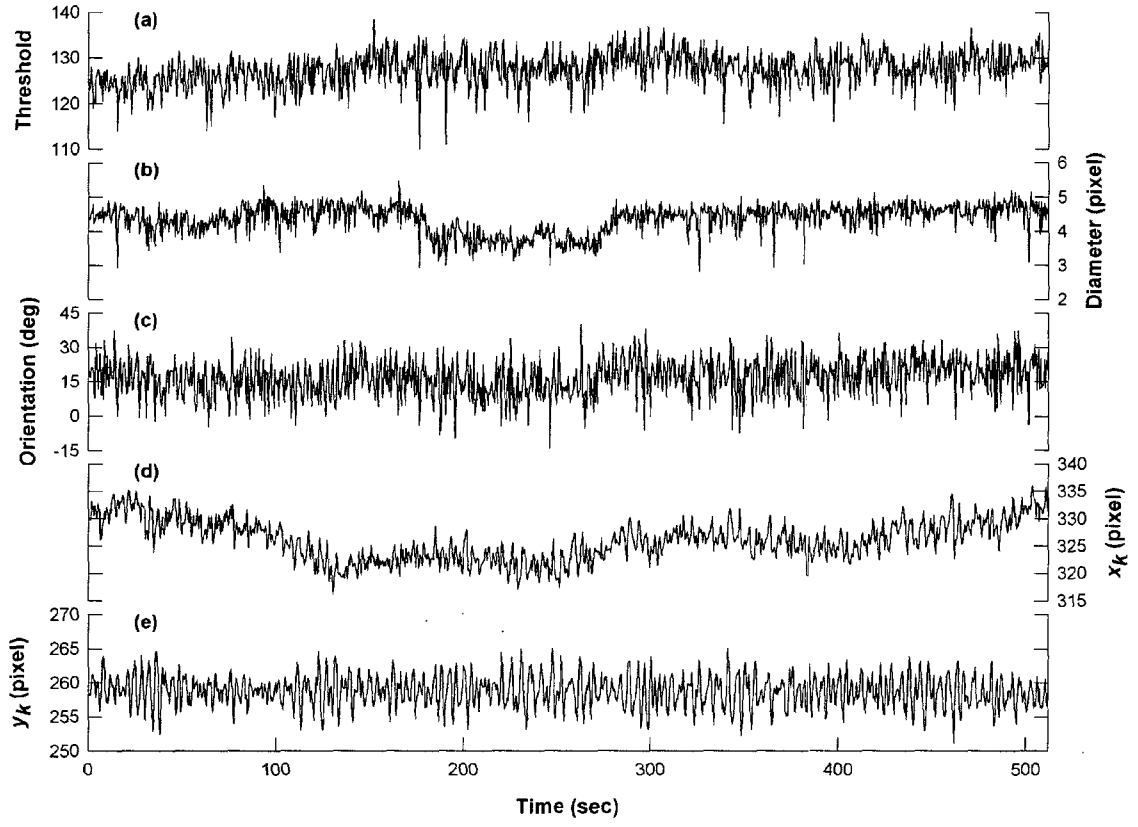

Fig. 6. Time series of image measurement parameters.

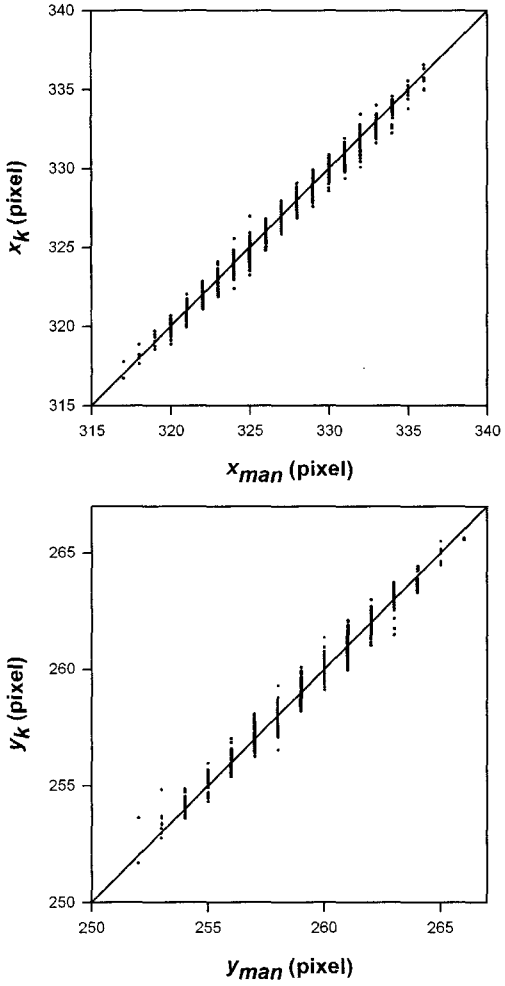

Fig. 7. Comparison of image coordinates between semi-automatic processing and manual processing.

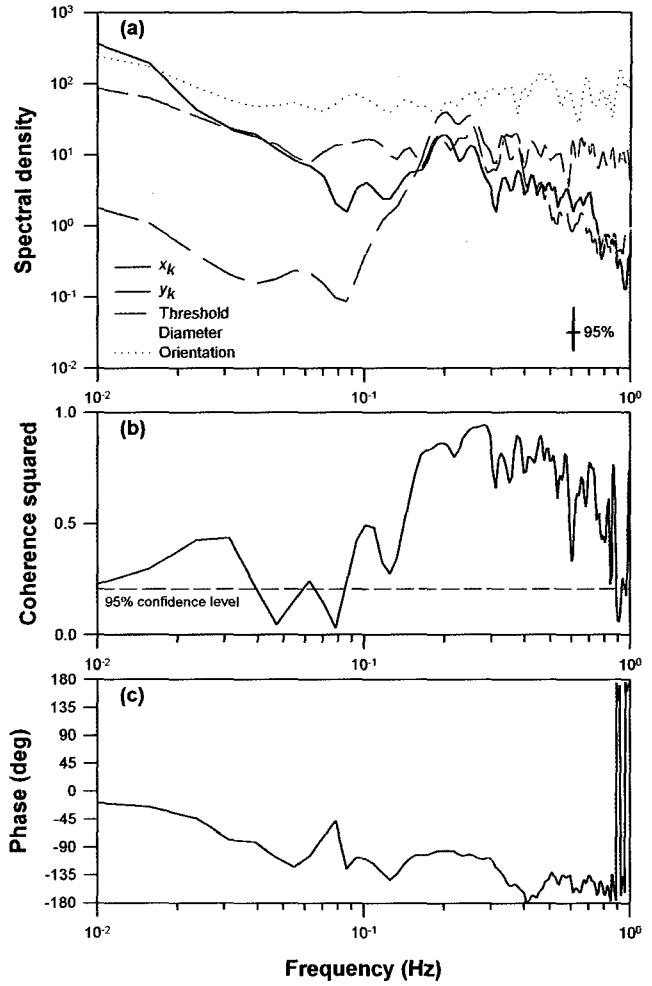

Fig. 8. Results of spectral analyses. (a) spectra of feature measurement parameters, (b) coherence and (c) phase relationship between xk and yk image coordinates.

feature measurement outputs within a run. Fluctuations of threshold and feature parameters such as diameter and orientation appear to be due to noise. On the contrary, those of centroid coordinates (xk, yk) show a regular motion superposed with much smaller scale fluctuations. For the horizontal motion, long-period variability is remarkable, leading to a greater range than the vertical motion. This is consistent with a set of buoy object locations forming an elliptical shape as shown in Fig. 5b and in a stacked image (see Fig. 6b in Kim, 2005).

The time-series of centroid image coordinates (xk, yk) are compared with those of pixel coordinates (x_{man}, y_{man}), which are manually extracted positions that are presumed to be a central location of buoy objects on a visual basis (Fig. 7). The manually extracted coordinates have one pixel resolution, whereas the centroid coordinates have much higher resolution due to subpixel interpolation as well as use of a continuous spatial coordinate system contrary to the discrete pixel coordinate system. Although with this discrepancy, there is fairly good agreement between the image processing and manual processing.

Spectral analysis shows that the spectra of threshold, diameter, and orientation (Fig. 8a) do not have any outstanding peaks, supporting the noise-like fluctuations of those parameters as depicted in Figs. 6a-c. On the other hand, the spectra of the xk and yk image coordinates show peaks around frequency of 0.2 Hz with minor undulations at higher frequencies (Fig. 8a). It is likely that the minor undulations are related to random variations in the size of the buoy object. At lower frequencies, energy

density of the xk image coordinate exceeds the spectral peak, explaining the long-period variation in the time-series of xk image coordinate (Fig. 6d). Likewise the coherence spectrum shows that the highest correlation between the xk and yk image coordinates occurs at the frequency band of 0.15 to 0.3 Hz (Fig. 8b). At this frequency band, the time-series of xk and yk image coordinates are 90° out of phase, *i.e.*, xk leads yk (Fig. 8c). As a result, the buoy object makes a counterclockwise trajectory. This means that incident waves approach obliquely from the upper right corner as observed in the video images (*e.g.* Fig. 3b).

4. Conclusions

Although this field experiment does not cover a wide range of wave and weather conditions, it gives valuable results for image processing of video images. It is obvious that data reduction of buoy motion images is not a simple but quite a complicated problem. The most important reason is that video monitoring is conducted in field environments where many aspects cannot be controlled. Time-varying properties of video images are found in the form of a noise, which can be easily manipulated by current image processing techniques. However, more advanced image processing is required to deal with interfering objects and missing cases.

Despite single video images, the time-series of image coordinates of buoy objects show that buoy motion follows water particle movement at the frequency of waves, indicating wave direction. This implies that buoy motion images have a great potential to be used for wave measurements.

Acknowledgements

This work was supported by Grant No. R01-2002-000-00273-0 from the Basic Research Program of the Korea Science & Engineering Foundation. Dr. J.Y. Jin (KORDI) and Dr. M.J. Lee (KRISO) are thanked for giving their kind comments to improve manuscript.

References

Holman, R.A., A.H. Sallenger, Jr., T.C. Lippmann, and J.W. Haines. 1993. The application of video image processing to the study of nearshore processes. *Oceanogr.*, **6**, 78-85.

Kim, B. O., Y.A. Park, I.S. Oh, B.K. Khim, and K.S. Choi. 1998. Beach profile estimation using a photogrammetry. *J. Kor. Soc. Oceanogr. (The Sea)*, **3**, 228-233. (In Korean)

Kim, B.O. 2005. Photography aided determination of video camera orientation in coastal environments. *J. Coastal Res.*, **SI42**, 352-362.

Lippmann, T.C. and R.A. Holman. 1989. Quantification of sand bar morphology: a video technique based on wave dispersion. *J. Geophys. Res.*, **94**, 995-1011.

MathWorks. 2001. Image processing toolbox user's guide. The MathWorks, Inc., Natick. 752 p.

Russ, J.C. 1990. Computer-assisted Microscopy: The measurement and analysis of images. Plenum Press, New York. 453 p.